The Investigational Drug VT-1129 is a Highly Potent Inhibitor of *Cryptococcus* species CYP51 but only Weakly Inhibits the Human Enzyme.

Andrew G.S. Warrilow[a], Josie E. Parker[a], Claire L. Price[a], W. David Nes[b], Edward P. Garvey[c], William J. Hoekstra[c], Robert J. Schotzinger[c], Diane E. Kelly[a] and Steven L. Kelly[a*]

Centre for Cytochrome P450 Biodiversity, Institute of Life Science, Swansea University Medical School, Swansea, Wales SA2 8PP, United Kingdom[a]; Center for Chemical Biology, Department of Chemistry and Biochemistry, Texas Tech University, Lubbock, Texas 79409-1061, USA[b]; Viamet Pharmaceuticals, Inc., Durham, NC 27703, USA[c]

Running title: VT-1129 and cryptococcal CYP51s.

Keywords: CYP51, VT-1129, *Cryptococcus*, azole antifungal.

[*]Corresponding author.

Mailing address: Institute of Life Science, Swansea University Medical School, Swansea, Wales SA2 8PP, United Kingdom. Phone: +44 1792 292207 Fax: +44 1792 503430 Email: s.l.kelly@swansea.ac.uk

Cryptococcosis is a life-threatening disease often associated with HIV infection. Three *Cryptococcus* species CYP51 enzymes were purified and catalyzed the 14α-demethylation of lanosterol, eburicol and obtusifoliol. The investigational agent VT-1129 bound tightly to all three CYP51 proteins (dissociation constant [K_d] range, 14 to 25 nM) with affinities similar to those of fluconazole, voriconazole, itraconazole, clotrimazole, and ketoconazole (K_d range, 4 to 52 nM), whereas VT-1129 bound weakly to human CYP51 (K_d, 4.53 μM). VT-1129 was as effective as conventional triazole antifungal drugs at inhibiting cryptococcal CYP51 activity (50% inhibitory concentration [IC_{50}] range, 0.14 to 0.20 μM), while it only weakly inhibited human CYP51 activity (IC_{50}, ~600 μM). Furthermore, VT-1129 weakly inhibited human CYP2C9, CYP2C19, and CYP3A4, suggesting a low drug-drug interaction potential. Finally, the cellular mode of action for VT-1129 was confirmed to be CYP51 inhibition, resulting in the depletion of ergosterol and ergosta-7-enol and the accumulation of eburicol, obtusifolione and lanosterol/obtusifoliol in the cell membranes.

Cryptococcosis is the most common systemic fungal infection in HIV/AIDS immunocompromised patients and is caused by the opportunistic basidiomycete yeast pathogen *Cryptococcus neoformans* (1) leading to infections of the lungs and brain. Meningoencephalitis is the most lethal manifestation of cryptococcosis with a life expectation of less than a month if untreated (2). Pathogenic *Cryptococcus* species cause disease in almost one million people annually with over 620,000 deaths and a third of all HIV/AIDS deaths are attributable to *Cryptococcus* species infection (1). Current treatment options are limited to a handful of drugs, namely initial induction therapy with a combination of amphotericin B and flucytosine followed by a maintenance regime of fluconazole (2). Even after administering the recommended treatment, three-month mortality rates of 10 to 20% are common (3, 4). In addition, adopting such treatment is costly and often impractical (with amphotericin B requiring intravenous administration), especially in developing countries where mortality rates can approach 100% (5, 6).

Three main *C. neoformans* varieties are observed in clinical infections. *C. neoformans var. grubii* (primarily serotype A), ubiquitous in the environment especially in soil, is globally distributed and is responsible for almost all cryptococcal infections in HIV/AIDS patients (6-8). *C. neoformans var. neoformans* (primarily serotype D) is less likely to cause severe infection and is more commonly found in Europe (4). *C. neoformans var. gattii* (primarily serotypes B and C), a tree-dwelling basidiomycete yeast primarily located in the tropics and sub-tropics with localized outbreaks in northeast America, is now considered a separate species (*C. gattii*) and is predominantly a primary pathogen infecting healthy (immunocompetent) individuals but will also infect immunocompromised patients if opportunity arises (9). Most

Cryptococcus infections of humans and nearly all infections of HIV/AIDS patients are caused by *C. neoformans var. grubii*, the most prevalent being the H99 strain, although *C. gattii* infection is increasing in prevalence, especially in North America and Africa (9). The taxonomy of *Cryptococcus* species is still evolving with Hagen *et al* (10) proposing that *C. neoformans var. neoformans* and *C. neoformans var. grubii* are separate species and that *C. gattii* consists of five distinct species based on phylogenetic analysis of 11 genetic loci.

Azole resistance, especially towards fluconazole, amongst *Cryptococcus* species in the clinic can be problematic due to prolonged maintenance treatment regimens (11). Increased azole tolerance in *Cryptococcus* species has been attributed to point mutations in CYP51, including G484S and Y145F (12, 13), increased expression levels of CYP51 and the transporter protein AFR1 (14) and the genome plasticity of *Cryptococcus* species post infection (15). Recently an *in silico* three-dimensional model of *C. neoformans* CYP51 has been published (16) with the aim of aiding new drug design. Because many of the marketed azole drugs are limited by a low therapeutic index (17), a drug with a higher therapeutic index might be able to combat resistant pathogens at plasma concentrations still below toxic levels.

In this study we compared the novel tetrazole antifungal VT-1129 (18, 19) (Fig. 1) with clinical azole antifungal drugs in terms of its potency and selectivity of binding to and inhibition of three recombinant cryptococcal CYP51 enzymes compared to human CYP51, and also to human CYPs that are critical xenobiotic-metabolizing enzymes. In addition, the *in vivo* mode of action for VT-1129 was demonstrated through sterol profile analysis.

MATERIALS AND METHODS

Construction of pCWori$^+$:*CneoCYP51*, pCWori$^+$:*CgruCYP51* and pCWori$^+$:*CgatCYP51* expression vectors. The *C. neoformans var. neoformans* CYP51 gene (CneoCYP51 - UniProtKB accession number Q5KQ65), the *C. neoformans var. grubii* CYP51 gene (CgruCYP51 - Q09GQ2) and the *C. gattii* CYP51 gene (CgatCYP51 - E6QZS1) were synthesized by Eurofins MWG Operon (Ebersberg, Germany) incorporating an *Nde*I restriction site at the 5' end and a *Hind*III restriction site at the 3' end of the genes cloned into the pBSIISK$^+$ plasmid. In addition the first eight amino acids were changed to 'MALLLAVF' (20) and a four-histidine extension (CATCACCATCAC) was inserted immediately before the stop codon. The cryptococcal CYP51 genes were excised by *Nde*I / *Hind*III restriction digestion followed by cloning into the pCWori$^+$ expression vector. Gene integrities were confirmed by DNA sequencing.

Heterologous expression and purification of recombinant cryptococcal CYP51 proteins. The pCWori$^+$:*CYP51* constructs were transformed into competent DH5α *E. coli* cells and expressed as previously described (21). Recombinant CYP51 proteins were isolated according to the method of Arase *et al* (22) except that 2% (wt/vol) sodium cholate was used in the sonication buffer and Tween-20 was omitted. The solubilized CYP51 proteins were purified by affinity chromatography using Ni^{2+}-NTA agarose as previously described (23, 21) prior to characterization. Human CYP51 with a deletion of 60 amino acids from the N-terminus (Δ60 truncated human CYP51) was expressed and purified as previously described (24) and was shown to be comparable to the full-length human CYP51 in terms of binding azole antifungal drugs. Protein purities were assessed by SDS polyacrylamide gel electrophoresis.

Cytochrome P450 protein determinations. Reduced carbon monoxide difference spectroscopy was performed (25) with carbon monoxide being passed through the cytochrome P450 solution prior to addition of sodium dithionite to the sample cuvette (light-path 10 mm). An extinction coefficient of 91 mM^{-1} cm^{-1} (26) was used to calculate cytochrome P450 concentrations from the absorbance difference between 447 and 490 nm. Absolute spectra were determined between 700 and 300 nm (light-path 10 mm). All spectral determinations were made using a Hitachi U-3310 UV/VIS spectrophotometer (San Jose, California).

Ligand binding studies. Stock 2.5 mM solutions of lanosterol, eburicol and obtusifoliol were prepared in 40% (wt/vol) (2-hydroxypropyl)-β-cyclodextrin (HPCD) using an ultrasonic bath. Sterol was progressively titrated against 5 μM CYP51 protein in a quartz semi-micro cuvette (light-path 4.5 mm) with equivalent amounts of 40% (wt/vol) HPCD added to the reference cuvette which also contained 5 μM CYP51. The difference in the spectrum between the absorbance at 500 and that at 350 nm was determined after each incremental addition of sterol (up to 75 μM). The sterol saturation curves were constructed from the difference spectra (difference in the A_{390} and A_{425}). The substrate dissociation constants (K_ds) were determined by non-linear regression (Levenberg-Marquardt algorithm) using the Michaelis-Menten equation.

Studies evaluating the binding of clotrimazole, fluconazole, voriconazole, itraconazole, ketoconazole and VT-1129 to the cryptococcal CYP51 proteins were performed as previously described (27, 21) using split-cuvettes with a 4.5-mm light path. Stock 0.1-mg-ml^{-1} solutions of the azole antifungal drugs were prepared in dimethyl sulfoxide (DMSO) and progressively titrated against 2 μM CYP51 in 0.1 M Tris-HCl (pH

8.1) and 25% (wt/vol) glycerol. The difference spectra between 500 and 350 nm were determined after each incremental addition of azole and binding saturation curves were constructed from the difference in the absorption at the peak and the absorption at the trough ($\Delta A_{peak\text{-}trough}$) against the azole concentration. The properties of VT-1129 binding with 5 μM recombinant human CYP51 was also determined (24). The K_ds of the enzyme-azole complex were determined by non-linear regression (Levenberg-Marquardt algorithm) using a rearrangement of the Morrison equation for tight ligand binding (28, 29). Tight binding occurs where the K_d for a ligand is similar or lower than the concentration of the enzyme present (30).

CYP51 reconstitution assays. Cryptococcal CYP51 reconstitution assays (31, 32) contained 0.5 μM CYP51, 1 μM *Aspergillus fumigatus* cytochrome P450 reductase (AfCPR1 - UniProtKB accession number Q4WM67), 50 μM C-14 methylated sterol substrate (lanosterol, eburicol, obtusifoliol), 50 μM dilaurylphosphatidylcholine, 4% (wt/vol) (2-hydroxypropyl)-β-cyclodextrin (HPCD), 0.4 mg ml^{-1} isocitrate dehydrogenase, 25 mM trisodium isocitrate, 50 mM NaCl, 5 mM $MgCl_2$ and 40 mM MOPS (morpholinepropanesulfonic acid; pH ~7.2). Assay mixtures were incubated at 37°C prior to initiation with 4 mM β-$NADPHNa_4$ followed by shaking at 37°C for 15 minutes. Human CYP51 reconstitution assays were performed as above except 0.5 μM soluble human CYP51 (24) and 2 μM human cytochrome P450 reductase (UniProtKB accession number P16435) were used and the reaction time reduced to 5 minutes at 37°C. Sterol metabolites were recovered by extraction with ethyl acetate followed by derivatization with *N*,*O*-bis(trimethylsilyl)trifluoroacetamide (BSTFA) and tetramethylsilane (TMCS) prior to analysis by gas chromatography (GC)-mass spectrometry (MS) (33).

Determinations of the 50% inhibitory concentration (IC_{50}s) were performed using 50 µM lanosterol as substrate in which various fluconazole, itraconazole, voriconazole and VT-1129 concentrations in 2.5 µl DMSO were added prior to incubation at 37°C and addition of β-$NADPHNa_4$.

***Cryptococcus* sterol analysis.** *C. neoformans var. neoformans* (strain ATCC MYA-565), *C. neoformans var. grubii* (strain ATCC 208821), and *C. gattii* (strain ATCC MYA-4071) were grown in MOPS buffered RPMI (0.165 M MOPS), pH 7.0, at 37°C and 200 rpm. MOPS buffered RPMI, pH 7.0, in the absence (1% vol/vol, DMSO control) or with fluconazole or VT-1129 was inoculated at a final concentration of 2.5×10^4 cells ml^{-1}. *C. neoformans var. neoformans* was grown in the presence of 0.2 µg ml^{-1} fluconazole or 0.0039 µg ml^{-1} VT-1129, *C. neoformans var. grubii* was grown in the presence of 0.4 µg ml^{-1} fluconazole or 0.0039 µg ml^{-1} VT-1129, and *C. gattii* was grown in the presence of 0.4 µg ml^{-1} fluconazole or 0.0078 µg ml^{-1} VT-1129. The cultures were grown for 2 days at 37°C, 200 rpm and nonsaponifiable lipids were extracted as previously reported (34).

Sterones were derivatized with methoxyamine-HCl by the addition of 200 µl of methoxyamine-HCl (2%, wt/vol, in anhydrous pyridine) and incubated for 30 min at 70°C. Samples were mixed with 2 ml of saturated NaCl, and the lipids extracted in three sequential 2-ml volumes of ethyl acetate. The combined ethyl acetate fractions were washed with 2-ml volumes of NaCl-saturated 0.1 M HCl, saturated NaCl, NaCl-saturated 5% (wt/vol) sodium bicarbonate solution and saturated NaCl. The samples were then dried over anhydrous magnesium sulphate and evaporated using a vacuum centrifuge. Sterols in the dried extracts were derivatized with 0.1 ml BSTFA-TMCS (99:1) and 0.3 ml anhydrous pyridine (2 h at 80°C) prior to analysis by GC-MS (33). Individual sterols

and sterones were identified by reference to the retention times, mass ions, and fragmentation patterns of sterol and sterone standards. Sterol composition was calculated using peak areas.

Inhibition of human liver CYP enzymes. *In vitro* studies determined the IC_{50}s of the test compounds for CYP2C9, CYP2C19, and CYP3A4 (with either midazolam or testosterone as substrates) in intact human liver microsomes. A separate series of incubation mixtures was prepared with each test compound at final concentration in reaction ranging from 0.0128 to 200 µM. Each incubation mixture contained pooled human liver microsomes at an assay concentration of 1 mg ml^{-1} microsomal protein (Life Technologies, Grand Island, NY) and metabolic substrates of isozymes for CYP2C9, CYP2C19, and CYP3A4 (diclofenac, omeprazole, and midazolam or testosterone, respectively) at their experimentally determined K_m concentrations. Active control wells contained microsomes, a substrate(s), and the test-compound diluent (i.e. DMSO-acetonitrile-phosphate buffer, 5:5:190) substituted for test compound solutions. The reaction was initiated by addition of an enzyme cofactor source (NADPH-regenerating solution; BD Biosciences, San Jose, CA) and the mixtures were incubated at 37°C. After 10 min, incubation mixtures were quenched with acetonitrile, mixed, and centrifuged. The supernatant was analyzed by high-performance liquid chromatography-tandem MS for the hydroxy metabolite of the substrates. Each product peak area was normalized to be represented as a percentage of the enzyme control average. The IC_{50} of each test compound was determined by fitting a 4-parameter logistical fit to the dose-response data and graphically determining the inhibitor concentration at 50% of the maximal enzymatic response.

Data analysis. All ligand binding experiments were performed in triplicate and curve-fitting of data performed using the computer program ProFit (version 6.1.12; QuantumSoft, Zurich, Switzerland). GC-MS data were analyzed using Thermo Xcalibur (version 2.2) software.

Chemicals. VT-1129 was provided by Viamet Pharmaceuticals, Inc. (Durham, USA). All other chemicals were obtained from Sigma Chemical Company (Poole, UK). Growth media, sodium ampicillin, IPTG (isopropyl-β-D-thiogalactopyranoside), and 5-aminolevulenic acid were obtained from Foremedium Ltd (Hunstanton, UK). Ni^{2+}-NTA agarose affinity chromatography matrix was obtained from Qiagen (Crawley, UK).

RESULTS

Expression and purification of cryptococcal CYP51 proteins. Following heterologous expression in *E. coli*, CneoCYP51, CgruCYP51 and CgatCYP51 were extracted by sonication with 2% (wt/vol) sodium cholate (22), which yielded 240 (±90), 160 (±50) and 290 (±80) nmoles per liter culture, as determined by carbon monoxide difference spectroscopy (25). Purification by chromatography on Ni^{2+}-NTA agarose resulted in 70%, 54% and 45% recoveries of native CneoCYP51, CgruCYP51 and CgatCYP51 proteins, respectively. SDS polyacrylamide gel electrophoresis confirmed the purity of the cryptococcal CYP51 proteins eluted on Ni^{2+}-NTA agarose to be greater than 90% when assessed by staining intensity, with apparent molecular weights being 55,000 to 58,000; the predicted molecular weights when the N-terminal modifications and the 4His C-terminal extensions are included were 62,708 for *C. neoformans* var. *neoformans*, 62,310 for *C. neoformans* var. *grubii*, and 62,689 for *C. gattii*.

Spectral properties of cryptococcal CYP51 proteins. The absolute spectra of the resting oxidized forms of all three CYP51 proteins (Fig. 2A) were typical for a low-spin ferric cytochrome P450 enzyme (23, 35) with α, β, Soret (γ) and δ spectral bands at 566, 536, 418 and 360 nm, respectively. Reduced carbon monoxide difference spectra (Fig. 2B) gave the red-shifted heme Soret peak at 447 nm, characteristic of P450 enzymes, indicating that all three CYP51 proteins were expressed in the native form.

Sterol binding properties of cryptococcal CYP51 proteins. Progressive titration with lanosterol, eburicol and obtusifoliol gave characteristic type I difference spectra for all three CYP51 proteins with a peak at 390 nm and a trough at 425 nm (Fig. 3). Type I binding spectra occur when the substrate or another molecule displaces the water molecule coordinated as the sixth ligand to the low-spin hexa-coordinated heme prosthetic group, causing the heme to adopt the high-spin penta-coordinated conformation (35). The cryptococcal CYP51 proteins had similar affinities for the three sterols (Table 1) with K_d values being 16 to 18 μM for lanosterol, 12 to 16 μM for eburicol and 12 to 21 μM for obtusifoliol. This result suggests that all three 14α-methylated sterols are potential substrates for the cryptococcal CYP51 proteins.

The sterol binding affinities of the three cryptococcal CYP51 proteins (K_d range, 12 to 21 μM) were similar to those reported for other CYP51 proteins. For example, K_d values for lanosterol and eburicol were 11 to 16 and 25 to 28 μM, respectively, with *Candida albicans* CYP51 (21), 11 and 13 μM, respectively, with *Mycosphaerella graminicola* CYP51 (36); and the K_d values were 0.5 to 18 μM for lanosterol with human CYP51 (24, 37, 38). However, the sterol K_d values obtained were 10- to 20-fold higher than those obtained for lanosterol with *Mycobacterium tuberculosis* CYP51 (1 μM) (23)

and for lanosterol and eburicol with *Trypanosoma cruzei* CYP51 (1.9 and 1.2 μM, respectively) (32).

CYP51 reconstitution assays. CYP51 assays using 50 μM sterol gave turnover numbers of 1.2 to 1.9 min^{-1} for lanosterol, 3.7 to 7.6 min^{-1} for eburicol and 3.5 to 4.5 min^{-1} for obtusifoliol (Table 1), confirming that all three cryptococcal CYP51 proteins readily catalyzed the 14α-demethylation of these three sterols. Both CneoCYP51 and CgruCYP51 displayed a substrate preference for eburicol over obtusifoliol and lanosterol, whilst CgatCYP51 displayed a substrate preference for obtusifoliol over eburicol and lanosterol. The ability of CgatCYP51, in particular, to readily demethylate obtusifoliol indicates a preference for a C-24-methylated sterol substrate.

Azole binding properties of CYP51 proteins. All five medical azole antifungal agents and the agent being investigated, VT-1129, bound tightly to all three cryptococcal CYP51 proteins, producing type II binding spectra. The binding spectra and saturation curves obtained for fluconazole and itraconazole (Fig. 4) and for VT-1129 (Fig. 5) are shown with a peak at ~429 nm and a trough at ~412 nm. Type II binding spectra are caused by the triazole ring N-4 (fluconazole, itraconazole, and voriconazole) or the imadazole ring N-3 (clotrimazole, ketoconazole) coordinating as the sixth ligand with the heme iron (39) to form the low-spin CYP51-azole complex, resulting in a 'red-shift' of the heme Soret peak. The interaction of VT-1129 with the heme ferric ion is through a terminal (N-3 or N-4) tetrazole nitrogen atom. CneoCYP51 bound the azole antifungal agents the strongest, with apparent K_d values of 4 to 11 nM (Table 1), followed by CgatCYP51 with apparent K_d values of 5 to 24 nM, and CgruCYP51 bound the azole antifungal agents the weakest, with apparent K_d values of 14 to 52 nM. None of the cryptococcal CYP51 enzymes appeared to be inherently resistant to azole antifungal

agents, as the range of K_d values observed (4 to 52 nM) was similar to those observed with *C. albicans* CYP51 (10 to 56 nM) (24), whereas *Aspegillus fumigatus* CYP51A appeared to be inherently resistant to fluconazole with an apparent K_d value of 11.9 μM (40). The affinity of VT-1129 binding to all three cryptococcal CYP51 proteins was strong (K_d range, 11 to 25 nM) and similar to that of the other five clinical azole antifungal agents examined, suggesting VT-1129 would be effective as a therapeutic agent against *Cryptococcus* species infections. The similar azole binding properties of the three cryptococcal CYP51 proteins agree with their close sequence homology with CneoCYP51 sharing 98% and 96% sequence identity with CgruCYP51 and CgatCYP51, respectively.

In contrast, VT-1129 bound relatively weakly to human CYP51 (Fig. 5) with an apparent K_d of 4.53 μM (Table 1). The interaction of VT-1129 with human CYP51 was atypical, as it gave rise to a red-shifted type I difference spectrum (peak at 410 nm and trough at 426 nm) rather than the expected type II difference spectrum normally observed for the interaction of azole antifungal agents with CYP51 proteins. This suggests that the mode of interaction of VT-1129 with the human CYP51 was different from that observed with the three cryptococcal CYP51 proteins. VT-1129 still perturbs the heme environment of human CYP51, as a difference spectrum was observed, though it was not through the azole nitrogen directly coordinating with the heme ferric ion. This altered interaction of VT-1129 with human CYP51 resulted in very weak inhibition of CYP51 activity in the CYP51 reconstitution assay (see below). The K_d values obtained for VT-1129 with the cryptococcal CYP51 enzymes were 180- to 410-fold lower than the K_d value obtained with the human homolog, confirming the high selectivity of VT-1129 for the fungal target enzyme. This compared favorably with the

findings for fluconazole and voriconazole, which gave K_d values that were 370- to 1,300-fold and 120- to 570-fold lower, respectively, for cryptococcal CYP51 enzymes than human CYP51. VT-1129 exhibited far greater selectivity than clotrimazole, ketoconazole, and itraconazole toward cryptococcal CYP51 enzymes than toward the human homolog, with clotrimazole, ketoconazole, and itraconazole exhibiting K_d values that were only 1.3- to 15-fold lower for the fungal CYP51 than for the human CYP51.

Azole IC_{50} determinations. IC_{50} determinations (Fig. 6) confirmed that all three cryptococcal CYP51 proteins tightly bound fluconazole, itraconazole voriconazole and VT-1129, giving rise to strong inhibition of the CYP51 demethylation of lanosterol. IC_{50}s of 0.14 to 0.20 μM (Table 1), which were obtained which were close to half the CYP51 concentration present in the assay system, were obtained. VT-1129 proved equally as effective at inhibiting cryptococcal CYP51 activity as the three other azole antifungal drugs, suggesting VT-1129 would be effective at combating *Cryptococcus* infections. In contrast, VT-1129 only weakly inhibited human CYP51 activity (IC_{50}, ~600 μM) (Fig. 7), in agreement with the weak perturbation of the heme environment of human CYP51 observed with VT-1129 (Fig. 5), whereas clotrimazole severely inhibited human CYP51 activity (IC_{50}, 1.9 μM). The IC_{50}s of VT-1129 observed for the cryptococcal CYP51 enzymes were 3,300- to 4,000-fold lower than that obtained with the human homolog (Table 1), again confirming high selectivity for the fungal target enzyme. This was comparable to the findings for fluconazole, where the IC_{50}s for the fungal CYP51 enzymes were 6,500- to 9,000-fold lower than those for human CYP51 and with the selectivity observed with fluconazole being significantly better than that observed with voriconazole and itraconazole (Table 1). The IC_{50}s of VT-1129 were more potent than the K_d values for binding to cryptococcal CYP51 enzymes, suggesting that the K_d values

323 calculated by the Morrison equation were an overestimate, in part due to the relatively
324 high CYP51 protein concentrations required for *in vitro* binding studies.

325 ***Cryptococcus* sterol content.** The treatment of *Cryptococcus* spp. with 0.2 to
326 0.4 μg ml^{-1} fluconazole and 0.0039 to 0.0078 μg ml^{-1} VT-1129 resulted in the
327 accumulation of eburicol (Table 2), obtusifolione and lanosterol/obtusifoliol. The
328 accumulation of CYP51 substrates is indicative of direct CYP51 inhibition in treated
329 cells. Both azole treatments resulted in the depletion of the post-CYP51 sterol
330 metabolites ergosta-7,22-dienol and ergosta-7-enol and the partial depletion of
331 ergosterol levels (Table 2), showing CYP51 inhibition. In these cellular experiments, VT-
332 1129 was significantly more potent than fluconazole, as VT-1129 caused greater
333 inhibition of cryptococcal CYP51 activity at a 50-fold lower concentration than
334 fluconazole (relative to the results observed with the DMSO control, VT-1129 caused
335 greater reductions in ergosterol levels than fluconazole at a 50-fold higher concentration,
336 and in all cases, the accumulation of the 14-methylated product showed that CYP51
337 was inhibited in cells; Table 2).

338 **Inhibition of human liver drug-metabolizing CYPs.** The inhibition of three
339 critical xenobiotic-metabolizing CYPs by the four approved azole drugs and VT-1129 is
340 shown in Table 3. The IC_{50}s of the marketed agents available in the literature (41-43)
341 agree well with those measured in this study. The imidazole-containing agent
342 clotrimazole was the most potent CYP inhibitor, inhibiting the activities of all CYPs at
343 sub- or low-micromolar concentrations. The three triazole-containing agents had
344 variable inhibitory potencies, with itraconazole potently inhibiting CYP3A4 with either
345 substrate (IC_{50}s, 0.08 and 0.13 μM), voriconazole inhibiting the activities of all CYPs with

a relatively tight range of potencies (IC_{50}s, 4 to 13 μM), and fluconazole showing a slightly broader range (IC_{50}s, 6 to 34 μM). In contrast, VT-1129 weakly inhibited the activities of each of these enzymes (IC_{50}s, 79 to 178 μM).

DISCUSSION

Sionov *et al* (14) demonstrated that *C. neoformans* strains are heteroresistant to fluconazole, with each strain yielding a sub-population that can survive in the presence of fluconazole concentrations well above the MIC values through disomy of chromosome 1, which duplicates the CYP51 and AFR1 transporter genes. The disomy of chromosome 1 coupled with reported G484S and Y145F CYP51 mutations (12, 13) increased CYP51 and AFR1 expression levels (14), and the genome plasticity post infection (15) may explain the divergent range of MIC values of fluconazole of 0.5 to 64 μg ml^{-1} reported for *Cryptococcus* spp. (44-47). The MIC values reported for voriconazole (0.008 to 0.5 μg ml^{-1}), itraconazole (0.015 to 0.5 μg ml^{-1}), and posaconazole (0.008 to 0.5 μg ml^{-1}) were lower and less variable than those reported for fluconazole (44-47), indicating the therapeutic efficacy of these triazole antifungals and their potential for use should fluconazole tolerance become problematic. However, as previously observed with *Candida* spp. and *Aspergillus* spp., it can be anticipated that tolerance against current triazole therapeutics will emerge in *Cryptococcus* spp.

New antifungal drug candidates for the treatment of systemic *Cryptococcus* infection which target CYP51 should ideally have high potency against the intended cryptococcal CYP51 target enzymes and minimal interaction with human CYP51 and other critical CYP enzymes, such as those that metabolize xenobiotics. VT-1129 meets

both these criteria by binding tightly to cryptococcal CYP51 enzymes (K_d range, 11 to 25 nM) with a high affinity similar to that of other pharmaceutical azole antifungal agents (K_d range, 4 to 52 nM) while binding weakly to the CYP51 of the human host *in vitro* (K_d, 4.53 μM). Binding studies (Fig. 4 and 5) provide useful preliminary information on a cyclized nitrogen-containing antifungal drug candidate's likely effectiveness at inhibiting CYP51 activity. However, only IC_{50} determinations using a CYP51 reconstitution assay system can determine the functional activity of each compound as a CYP51 inhibitor. IC_{50} determinations confirmed that VT-1129 is a strong inhibitor of cryptococcal CYP51 activity, consistent with tight binding inhibition, but only weakly inhibits human CYP51 (13% inhibition at 150 μM VT-1129). The selectivity of VT-1129 for the cryptococcal CYP51 protein over the human homolog was ~3,300-fold in terms of inhibiting CYP51 catalysis, and VT-1129 was as effective as conventional triazole antifungal drugs at inhibiting cryptococcal CYP51 activity. VT-1129's selectivity for inhibiting cryptococcal CYP51 was similarly high compared to its selectivity for inhibiting key human xenobiotic-metabolizing CYPs, suggesting a low potential for clinical drug-drug interactions.

Sterol profile analysis confirmed that VT-1129 inhibited cryptococcal CYP51 activity in whole cells, resulting in the depletion of ergosterol and ergosta-7-enol from the cell membranes and the accumulation of the 14-methylated compounds eburicol and lanosterol/obtusifoliol and obtusifolione. In a separate study measuring a large number of *Cryptococcus* species isolates and using 50% inhibition as the endpoint, the MIC_{90} of VT-1129 was 0.060 μg ml^{-1} for 180 isolates of *C. neoformans* and 0.25 μg ml^{-1} for 321 isolates of *C. gattii* (19), confirming that VT-1129 is a potent inhibitor of *Cryptococcus* growth. In both studies, VT-1129 was a more potent inhibitor of *Cryptococcus* CYP51 than fluconazole. In addition, VT-1129 retains all or most of its antifungal potency

against 50 Ugandan clinical isolates of *C. neoformans* with elevated fluconazole MIC values (48). This potency coupled with its excellent selectivity for fungal rather than human CYP enzymes shown here supports VT-1129 as a good candidate for the treatment of systemic *Cryptococcus* infections. Given the unmet need for more potent drugs for the treatment of cryptococcosis, especially in sub-Saharan Africa, further assessments in clinical trials are warranted, with VT-1129 Phase 1 studies with healthy volunteers now being underway.

ACKNOWLEDGMENT

We are grateful to the Engineering and Physical Sciences Research Council National Mass Spectrometry Service Centre at Swansea University and Marcus Hull for assistance with GC-MS analyses.

This work was supported in part by the European Regional Development Fund/Welsh Government funded BEACON research program (Swansea University), the National Science Foundation of the United States (grant NSF-MCB-09020212 awarded to W. David Nes, Texas Tech University), and by Viamet Pharmaceuticals, Inc. (Durham, NC 27703, USA).

FUNDING INFORMATION

This work, including the efforts of W. David Nes, was funded by NSF (NSF-MCB-09020212).

REFERENCES

1. **Park BJ, Wannemuehler KA, Marston BJ, Govender N, Pappas PG, Chiller TM.** 2009. Estimation of the current global burden of cryptococcal meningitis among persons living with HIV/AIDS. Aids. **23:**525-530.

2. **Bicanic T, Harrison TS.** 2004. Cryptococcal meningitis. Br. Med. Bull. **72:**99-118.

3. **Lortholary O, Poizat G, Zeller V, Neuville S, Boibieux A, Alvarez M, Dellamonica P, Botterel F, Dromer F, Chene G, and the French Cryptococcosis study group.** 2006. Long-term outcome of AIDS-associated cryptococcosis in the era of combination antiretroviral therapy. Aids. **20:**2183-2191.

4. **Dromer F, Mathoulin-Pelissier S, Launay O, Lortholary O.** 2007. Determinants of disease presentation and outcome during cryptococcosis: the Crypto A/D study. PLoS Med. **4:**e21.

5. **Mwaba P, Mwansa J, Chintu C, Pobee J, Scarborough M, Portsmouth S, Zumla A.** 2001. Clinical presentation, natural history, and cumulative death rates of 230 adults with primary cryptococcal meningitis in Zambian AIDS patients treated under local conditions. Postgrad. Med. J. **77:**769-773.

6. **French N, Gray K, Watera C, Nakiyingi J, Lugada E, Moore M, Lalloo D, Whitworth JAG, Gilks CF.** 2002. Cryptococcal infection in a cohort of HIV-1-infected Ugandan aldults. Aids. **16:**1031-1038.

7. **Canteros CE, Brundy M, Rodero L, Perrotta D, Davel G.** 2002. Distribution of *Cryptococcus neoformans* serotypes associated with human infections in Argentina. Rev. Argent. Microbiol. **34:**213-218.

8. **Banerjee U, Datta K, Casadevall A.** 2004. Serotype distribution of *Cryptococcus neoformans* in patients in a tertiary care center in India. Med. Mycol. **242:**181-186.

9. **Byrnes EJ, Bartlett KH, Perfect JR, Heitman J.** 2011. *Cryptococcus gattii*: an emerging fungal pathogen infecting humans and animals. Microbes Infect. **13:**895-907.

10. **Hagen F, Khayhan K, Theelen B, Kolecka A, Polacheck I, Sionev E, Falk R, Parnmen S, Lumbsch HT, Boekhout T.** 2015. Recognition of seven species in the *Cryptococcus gattii* / *Cryptococcus neoformans* species complex. Fungal Genet. Biol. **78:**16-48.

11. **Perfect JR, Cox GM.** Drug resistance in *Cryptococcus neoformans*. 1999. Drug Resist. Update. **2:**259-269.

12. **Rodero L, Mellado E, Rodriguez AC, Salve A, Guelfand L, Cahn P, Cuenca-Estrella M, Davel G, Rodriguez-Tudela JL.** 2003. G484S amino acid substitution in lanosterol 14-α demethylase (ERG11) is related to fluconazole resistance in a recurrent *Cryptococcus neoformans* clinical isolate. Antimicrob Agents Chemother **47:**3653-3656.

13. **Sionov E, Chang YC, Garraffo HM, Dolan MA, Ghannoum MA, Kwon-Chung KJ.** 2012. Identification of a *Cryptococcus neoformans* cytochrome P450 lanosterol 14α-demethylase (Erg11) residue critical for differential susceptibility between fluconazole/voriconazole and itraconazole/posaconazole. Antimicrob. Agents Chemother. **56:**1162-1169.

14. **Sionov E, Lee H, Chang YC, Kwon-Chung KJ.** 2010. *Cryptococcus neoformans* overcomes stress of azole drugs by formation of disomy in specific multiple chromosomes. PLoS Pathogens. **6:**e1000848.

15. **Hu G, Wang J, Choi J, Jung WH, Liu I, Litvintseva AP, Bicanic T, Aurora R, Mitchell TG, Perfect JR, Kronstad JW.** 2011. Variation in chromosome copy number influences the virulence of *Cryptococcus neoformans* and occurs in isolates from AIDS patients. BMC Genomics. **12:**526.

16. **Sheng C, Miao Z, Ji H, Yao J, Wang W, Che X, Dong G, Lu J, Guo W, Zhang W.** 2009. Three-dimensional model of lanosterol 14α-demethylase from *Cryptococcus neoformans*: active-site characterization and insights into azole binding. Antimicrob. Agents Chemother. **53:**3487-3495.

17. **Suzuki Y, Tokimatsu I, Sato Y, Kawasaki K, Sato Y, Goto T, Hashinaga K, Itoh H, Hiramatsu K, Kadota J.** 2013. Association of sustained high plasma trough concentration of voriconazole with the incidence of hepatotoxicity. Clin. Clim. Acta. **424:**119-122.

18. **Hoekstra WJ, Garvey EP, Moore WR, Rafferty SW, Yates CM, Schotzinger RJ.** 2014. Design and optimization of highly-selective fungal CYP51 inhibitors. Bioorg. Med. Chem. Lett. **24:**3455-3458.

19. **Lockhart SR, Fothergill AW, Iqbal N, Bolden CB, Grossman NT, Garvey EP, Brand SR, Hoekstra WJ, Schotzinger RJ, Ottinger E, Patterson TF, Wiederhold NP.** 2016. The investigational fungal Cyp51 inhibitor VT-1129 demonstrates potent in vitro activity against *Cryptococcus neoformans* and *Cryptococcus gattii*. Antimicrob. Agents Chemother. In press AAC.02770-15.

20. **Barnes HJ, Arlotto MP, Waterman MR.** 1991. Expression and enzymatic activity of recombinant cytochrome P450 17α-hydroxylase in *Escherichia coli*. Proc. Natl. Acad. Sci. USA. **88:**5597-5601.

21. **Warrilow AGS, Martel CM, Parker JE, Melo N, Lamb DC, Nes D, Kelly DE, Kelly SL.** 2010. Azole binding properties of *Candida albicans* sterol 14-α demethylase (CaCYP51). Antimicrob. Agents Chemother. **54:**4235-4245.

22. **Arase M, Waterman MR, Kagawa N.** 2006. Purification and characterization of bovine steroid 21-hydroxylase (P450c21) efficiently expressed in *Escherichia coli*. Biochem. Biophys. Res. Com. **344:**400-405.

23. **Bellamine A, Mangla AT, Nes WD, Waterman MR. 1999.** Characterisation and catalytic properties of the sterol 14α-demethylase from *Mycobacterium tuberculosis*. Proc. Natl. Acad. Sci. USA. **96:**8937-8942.

24. **Warrilow AGS, Parker JE, Kelly DE, Kelly SL.** 2013. Azole affinity of sterol 14α-demethylase (CYP51) enzymes from *Candida albicans* and *Homo sapiens*. Antimicrob. Agents Chemother. **57:**1352-1360.

25. **Estabrook RW, Peterson JA, Baron J, Hildebrandt AG.** 1972. The spectrophotometric measurement of turbid suspensions of cytochromes associated with drug metabolism, p 303-350. In: Chignell CF (ed), Methods in Pharmacology, vol 2, Appleton-Century-Crofts, New York, NY.

26. **Omura T, Sato R.** 1964. The carbon monoxide-binding pigment of liver microsomes. J. Biol. Chem. **239:**2379-2385.

27. **Lamb DC, Kelly DE, Waterman MR, Stromstedt M, Rozman D, Kelly SL.** 1999. Characteristics of the heterologously expressed human lanosterol 14α-

demethylase (other names: P45014DM, CYP51, P45051) and inhibition of the purified human and *Candida albicans* CYP51 with azole antifungal agents. Yeast **15:**755-763.

28. **Lutz JD, Dixit V, Yeung CK, Dickmann LJ, Zelter A, Thatcher JA, Nelson WL, Isoherranen N.** 2009. Expression and functional characterization of cytochrome P450 26A1, a retinoic acid hydroxylase. Biochem. Pharmacol. **77:**258-268.

29. **Morrison JF.** 1969. Kinetics of the reversible inhibition of enzyme-catalysed reactions by tight-binding inhibitors. Biochim. Biophys. Acta – Enzymol. **185:**269-286.

30. **Copeland RA.** 2005. Evaluation of enzyme inhibitors in drug discovery: a guide for medicinal chemists and pharmacologists, p 178-213, Wiley-Interscience, New York, NY.

31. **Lepesheva GI, Ott RD, Hargrove TY, Kleshchenko YY, Schuster I, Nes WD, Hill GC, Villalta F, Waterman MR.** 2007. Sterol 14α-demethylase as a potential target for antitrypanosomal therapy: enzyme inhibition and parasite cell growth. Chem. Biol. **14:**1283–1293.

32. **Lepesheva GI, Zaitseva NG, Nes WD, Zhou W, Arase M, Liu J, Hill GC, Waterman MR.** 2006. CYP51 from *Trypanosoma cruzi*: a phyla-specific residue in the B' helix defines substrate preferences of sterol 14α-demethylase. J. Biol. Chem. **281:**3577–3585.

33. **Parker JE, Warrilow AGS, Cools HJ, Fraaije BA, Lucas JA, Rigdova K, Griffiths WJ, Kelly DE, Kelly SL.** 2011. Prothioconazole and prothioconazole-desthio activity against *Candida albicans* sterol 14α-demethylase (CaCYP51). Appl. Environ. Microbiol. **79:**1639-1645.

34. **Kelly SL, Lamb DC, Corran AJ, Baldwin BC, Kelly DE.** 1995. Mode of action and resistance to azole antifungals associated with the formation of 14α-methylergosta-8,24(28)-dien-3β,6α-diol. Biochem. Biophys. Res. Comm. **207:**910-915.

35. **Jefcoate CR.** 1978. Measurement of substrate and inhibitor binding to microsomal cytochrome P-450 by optical-difference spectroscopy. Methods Enzymol. **52:**258-279.

36. **Parker JE, Warrilow AGS, Cools HJ, Martel CM, Nes WD, Fraaije BA, Lucas JA, Kelly DE, Kelly SL.** 2011. Mechanism of binding of prothioconazole to *Mycosphaerella graminicola* CYP51 differs from that of other azole antifungals. Appl. Environ. Microbiol. **77:**1460-1465.

37. **Lepesheva GI, Nes WD, Zhou W, Hill GC, Waterman MR.** 2004. CYP51 from *Trypanosoma brucei* is obtusifoliol-specific. Biochemistry **43:**10789–10799.

38. **Strushkevich N, Usanov SA, Park HW.** 2010. Structural basis of human CYP51 inhibition by antifungal azoles. J. Mol. Biol. **397:**1067-1078.

39. **Jefcoate CR, Gaylor JL, Calabrese RL.** 1969. Ligand interactions with cytochrome P450. I. Binding of primary amines. Biochemistry **8:**3455-3463.

40. **Warrilow AGS, Melo N, Martel CM, Parker JE, Nes D, Kelly DE, Kelly SL.** 2010. Expression, purification, and characterization of *Aspergillus fumigatus* sterol 14-α demethylase (CYP51) isoenzymes A and B. Antimicrob. Agents Chemother. **54:**4225-4234.

41. **Niwa T, Shiraga T, Takagi A.** 2005. Effect of antifungal drugs on cytochrome P450 (CYP) 2C9, CYP2C19, and CYP3A4 activities in human liver microsomes. Biol. Pharm. Bull. **28:**1805-1808.

42. **Zhang S, Pillai VC, Mada SR, Strom S, Venkataramanan R.** 2012. Effect of voriconazole and other azole antifungal agents on CYP3A activity and metabolism of tacrolimus in human liver microsomes. Xenobiotica **42:**409-416.

43. **Zhang W, Ramamoorthy Y, Kilicarslan T, Nolte H, Tyndale RF, Sellers EM.** 2002. Inhibition of cytochromes P450 by antifungal imidazole derivatives. Drug Met. Disp. **30:**314-318.

44. **Trilles L, Meyer W, Wanke B, Guarro J, Lazera M.** 2012. Correlation of antifungal susceptibility and molecular type within the *Cryptococcus neoformans* / *C. gattii* species complex. Med. Mycol. **50:**328-332.

45. **Pfaller MA, Castanheira M, Messer SA, Moet GJ, Jones RN.** 2011. Echinocandin and triazole antifungal susceptibility profiles for *Candida* spp., *Cryptococcus neoformans*, and *Aspergillus fumigatus*: application of new CLSI clinical breakpoints and epidemiologic cutoff values to characterize resistance in the SENTRY antimicrobial surveillance program (2009). Diag. Microbiol. Infect. Dis. **69:**45-50.

46. **Bertout S, Drakulovski P, Kouanfack C, Krasteva D, Ngouana T, Dunyach-Remy C, Dongsta J, Aghokeng A, Delaporte E, Koulla-Shiro S, Reynes J, Mallie M.** 2012. Genotyping and antifungal susceptibility testing of *Cryptococcus neoformans* isolates from Cameroonian HIV-positive adult patients. Clin. Microbiol. Infect. **19:**763-769.

47. **Lockhart SR, Iqbal N, Bolden CB, DeBess EE, Marsden-Haug N, Worhle R, Thakur R, Harris JR.** 2012. Epidemiologic cutoff values for triazole drugs in *Cryptococcus gattii*: correlation of molecular type and in vitro susceptibility. Diag. Microbiol. Infect. Dis. **73:**144-148.

48. **Vedula P, Smith K, Boulware DR, Meya DB, Garvey EP, Hoekstra WJ, Schotzinger RJ, Nielsen K.** 2015. Activity of VT-1129 against *Cryptococcus neoformans* clinical isolates with high fluconazole MICs. 2015 Interscience Conference on Antimicrobial Agents and Chemotherapy, San Diego, CA. Poster F-763a.

587 **TABLE 1** Ligand binding affinities, azole IC_{50}s, and turnover numbers for CYP51

	K_d (nM)							
	Sterols			Azoles				
CYP51	Lanosterol	Eburicol	Obtusifoliol	Clotrimazole	Fluconazole	Itraconazole	Ketoconazole	Vo
CneoCYP51	16,300 ±2,800	13,000 ±1,200	16,800 ±2,100	4 ±3	9 ±5	7 ±3	6 ±2	4 ±
CgruCYP51	17,300 ±900	11,700 ±600	12,200 ±3,000	44 ±18	52 ±15	42 ±11	32 ±15	14
CgatCYP51	17,500 ±1,900	15,800 ±1,300	20,600 ±1,000	11 ±4	24 ±9	6 ±2	5 ±2	19
HsapCYP51	18,400 ±1,500[b]			55 ±5[b]	30,400 ±4,100[b]	92 ±7[b]	42 ±16[a]	2,2

588 [a] HsapCYP51, *Homo sapiens* CYP51.
589 [b] Values were taken from Warrilow *et al*. (24).
590 [c] Thirteen percent inhibition was observed in the presence of 150 μM VT-1129.
591
592
593
594 **TABLE 1** (Continued)

	IC_{50} (μM)					Turnover no. (min^{-1})	
CYP51	Clotrimazole	Fluconazole	Itraconazole	Voriconazole	VT-1129	Lanosterol	Eburic
CneoCYP51		0.17	0.17	0.17	0.16	1.4 ±0.2	6.1 ±0
CgruCYP51		0.2	0.19	0.2	0.18	1.9 ±0.3	7.6 ±0
CgatCYP51		0.14	0.16	0.16	0.15	1.2 ±0.2	3.7 ±0
HsapCYP51	1.9	~1,300[b]	70[b]	112	~600[c]	22.7 ±4.8	

595
596

597 **TABLE 2** Sterol profiles of *Cryptococcus* spp.

Sterols	Sterol composition (%) with the indicated treatment [a]						
	C. neoformans var. neoformans			*C. neoformans var. grubii*			*C. gattii*
	DMSO	+FLUC	+VT1129	DMSO	+FLUC	+VT1129	DMSO
Ergosta-5,7,22,24(28)-tetraenol	-	1.2 ±0.3	5.0 ±0.5	2.5 ±1.4	2.1 ±1.6	2.3 ±0.3	-
Ergosta-5,8,22-trienol	-	1.0 ±0.0	3.7 ±0.3	-	-	-	-
Ergosterol	60.6 ±2.5	42.2 ±0.7	11.5 ±3.9	43.9 ±4.3	34.1 ±3.6	18.7 ±0.6	49.3 ±9.7
Ergosta-7,22-dienol	7.4 ±0.4	-	-	9.3 ±1.1	-	-	10.8 ±6.0
Fecosterol (E8,24(28))	-	-	-	-	-	-	1.0 ±0.9
Ergosta-8-enol	-	1.6 ±0.4	-	-	-	-	-
Ergosta 5,7 dienol	-	-	-	-	-	-	3.0 ±0.6
Ergosta-7-enol	25.3 ±1.0	-	-	28.8 ±0.5	-	-	30.2 ±6.6
Eburicone	-	-	-	-	-	-	-
Lanosterol / Obtusifoliol	-	3.7 ±0.9	4.4 ±0.2	1.7 ±1.1	10.9 ±2.1	4.9 ±0.0	-
4-methyl fecosterol	-	-	-	2.5 ±0.4	-	-	-
Obtusifolione	-	35.9 ±1.8	17.1 ±1.0	-	22.1 ±1.5	24.5 ±0.6	-
Eburicol	1.5 ±0.8	12.8 ±0.7	55.8 ±5.7	6.8 ±2.0	30.0 ±2.1	49.1 ±1.1	3.1 ±2.5
4,4-dimethyl-ergosta-8,24(28)-dienol	-	-	-	4.0 ±0.8	-	-	-

598 [a] Mean values from three replicates ± standard deviations are shown. FLUC, fluconazole.
599

TABLE 3 Inhibition of human liver CYPs by fungal CYP51 inhibitors.

Inhibitor	IC_{50} (μM) [a]			
	2C9	2C19	3A4 [b]	3
Clotrimazole	1.4 (0.1)	0.6 (0.2)	0.03 (0.01)	0
Fluconazole	34 (10)	13 (9)	32 (5)	6
Itraconazole	80 (28)	78 (31)	0.08 (0.02)	0
Voriconazole	10 (5)	10 (4)	13 (4)	3
VT-1129	87 (21)	110 (80)	79 (23)	1

[a] Values are averages of 2 to 4 separate determinations with standard deviations in parenthesizes.
[b] Testosterone as substrate.
[c] Midazolam as substrate.

604

Fluconazole

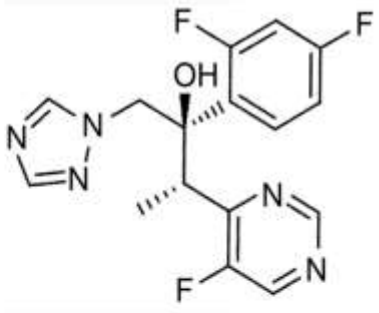

Voriconazole

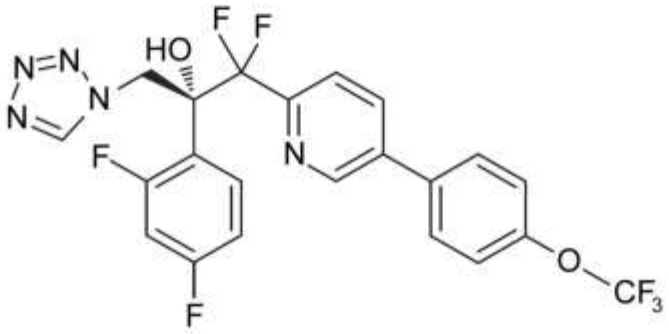

VT-1129

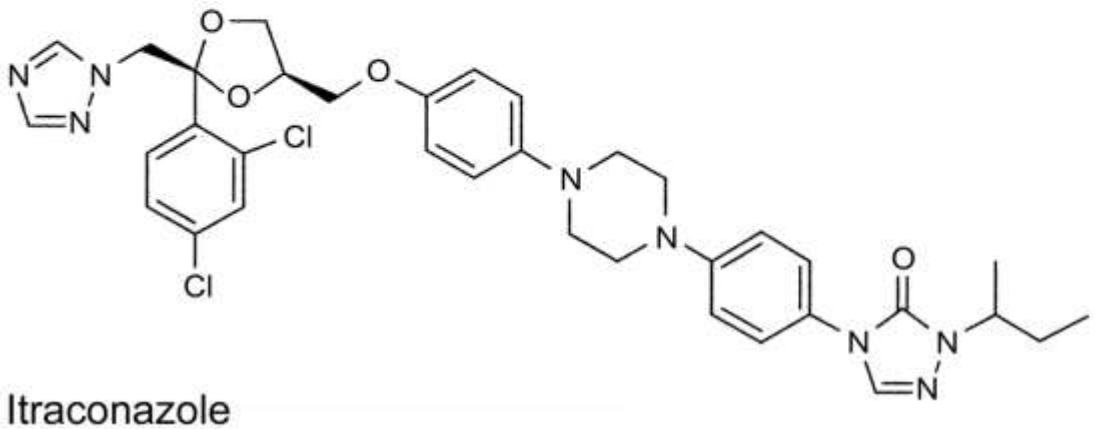

Itraconazole

605

606 **FIG 1** Chemical structures of the azole antifungals used for IC_{50} studies. The chemical

607 structures of fluconazole (molecular weight, 306), voriconazole (molecular weight, 349),

608 VT-1129 (molecular weight, 513), and itraconazole (molecular weight, 706) are shown.

609

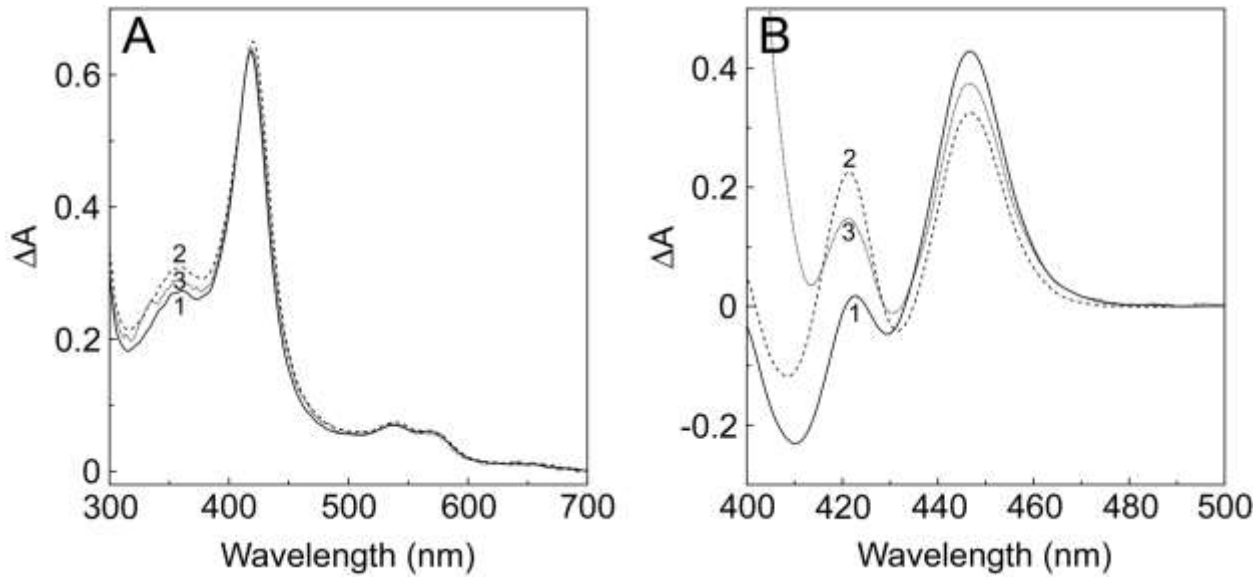

FIG 2 Absolute and reduced carbon monoxide spectra of cryptococcal CYP51 proteins. Absolute spectra in the oxidised resting state (A) and reduced carbon monoxide difference spectra (B) were determined using 5 μM solutions of purified CneoCYP51 (line 1), CgruCYP51 (line 2), and CgatCYP51 (line 3). Spectral determinations were made using quartz semimicrocuvettes with a path length of 10 mm.

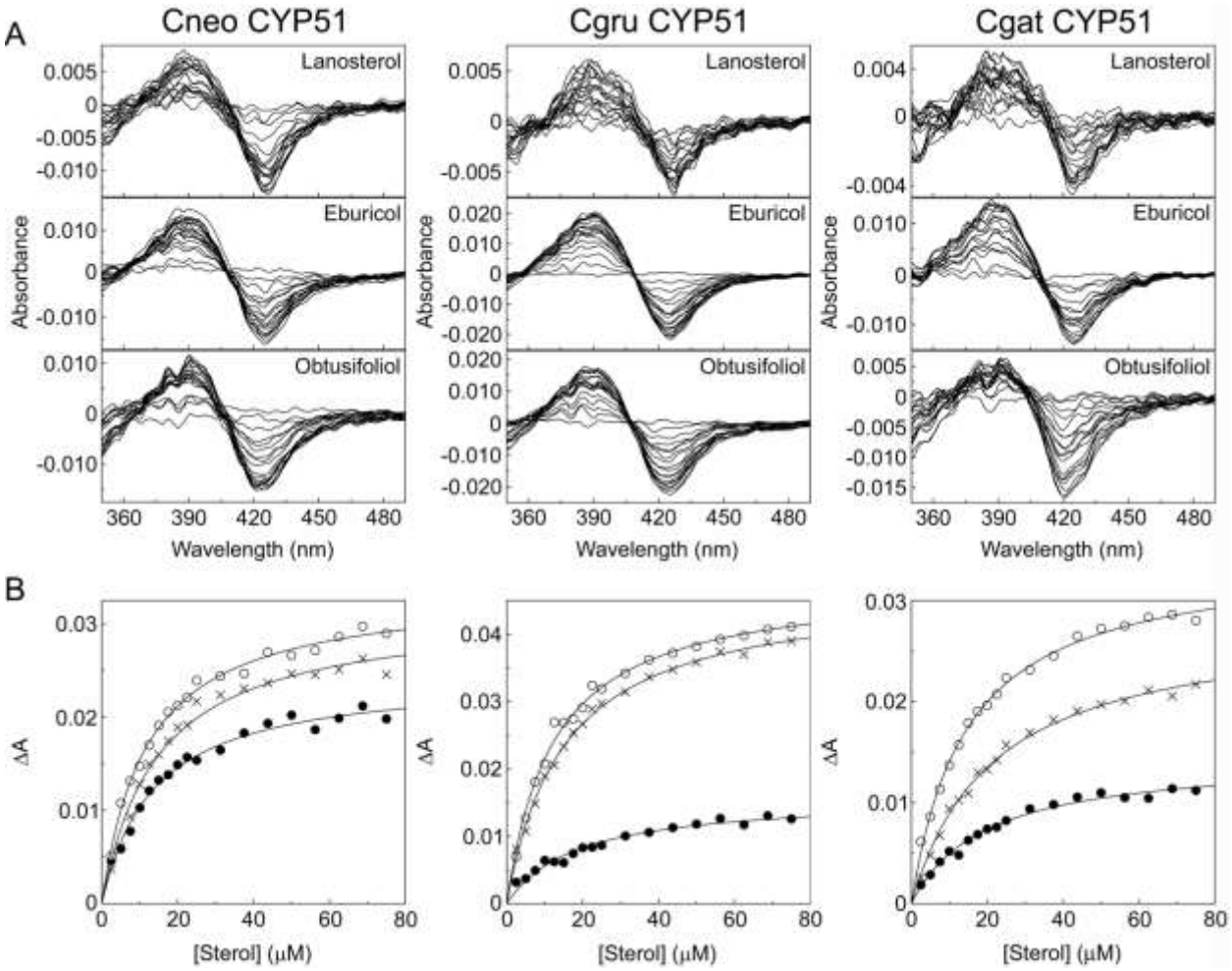

FIG 3 Sterol binding properties of cryptococcal CYP51 proteins. (A) Absorbance difference spectra were measured during the progressive titration of 5 μM CYP51 proteins with lanosterol, eburicol and obtusifoliol. (B) Sterol saturation curves were constructed for lanosterol (filled circles), eburciol (hollow circles) and obtusifoliol (crosses) with the CYP51 proteins from the difference between the A_{390} and A_{425} of the type I binding spectra observed and were fitted using the Michaelis-Menten equation.

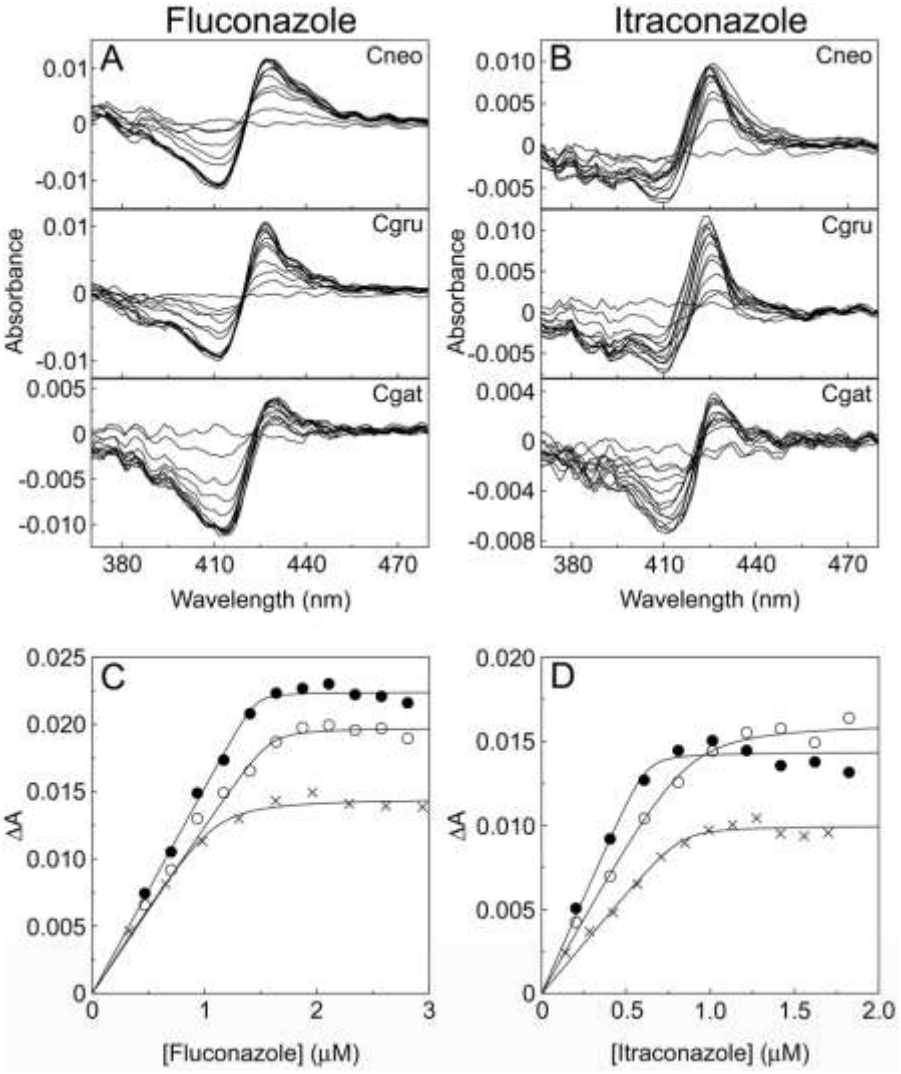

FIG 4 Azole binding properties of cryptococcal CYP51 proteins. Fluconazole and itraconazole were progressively titrated against 2 μM CneoCYP51, CgruCYP51, and CgatCYP51. (A and B) The resultant type II difference spectra obtained with fluconazole (A) and itraconazole (B) are shown. (C and D) Fluconazole (C) and itraconazole (D) saturation curves were constructed from the $\Delta A_{peak\text{-}trough}$ of the type II binding spectra observed for CneoCYP51 (solid circles), CgruCYP51 (hollow circles), and CgatCYP51 (crosses). A rearrangement of the Morrison equation was used to fit the tight ligand binding observed. All experiments were performed in triplicate, although the results of only one replicate are shown.

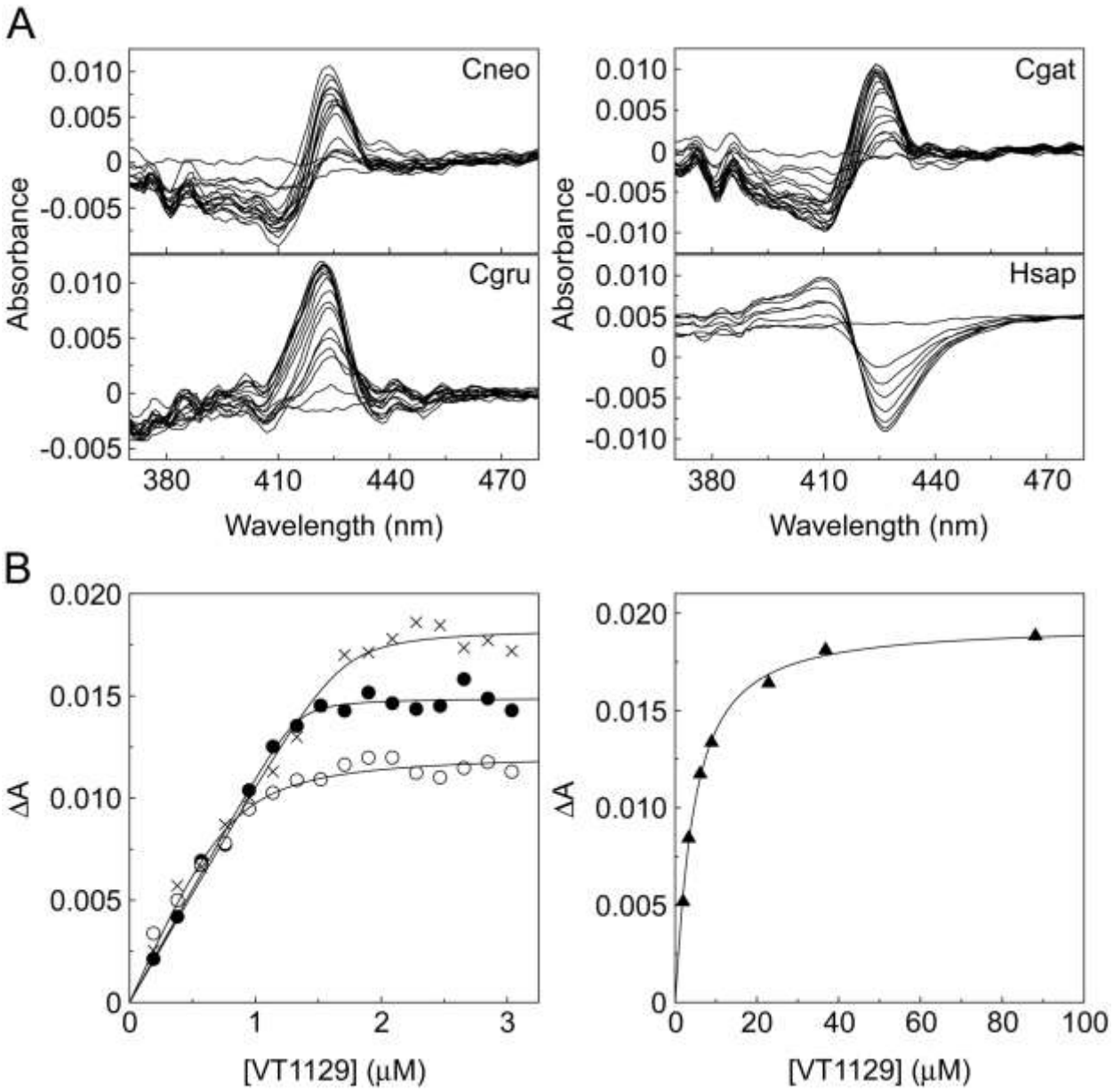

FIG 5 VT-1129 binding properties of cryptococcal and human CYP51 proteins. VT-1129 was progressively titrated against 4 μM CneoCYP51, CgruCYP51, and CgatCYP51 and 5 μM human (*Homo sapiens*) CYP51 (Hsap). (A) The resultant type II difference spectra obtained with the three cryptococcal CYP51 proteins and the red-shifted type I difference spectrum with human CYP51 are shown. (B) Saturation curves were

constructed from the $\Delta A_{peak\text{-}trough}$ of the type II binding spectra observed for CneoCYP51 (solid circles), CgruCYP51 (hollow circles), CgatCYP51 (crosses), and the red-shifted type I binding spectrum observed for human CYP51 (solid triangles). A rearrangement of the Morrison equation was used to fit the tight ligand binding observed. All experiments were performed in triplicate, although the results of only one replicate are shown.

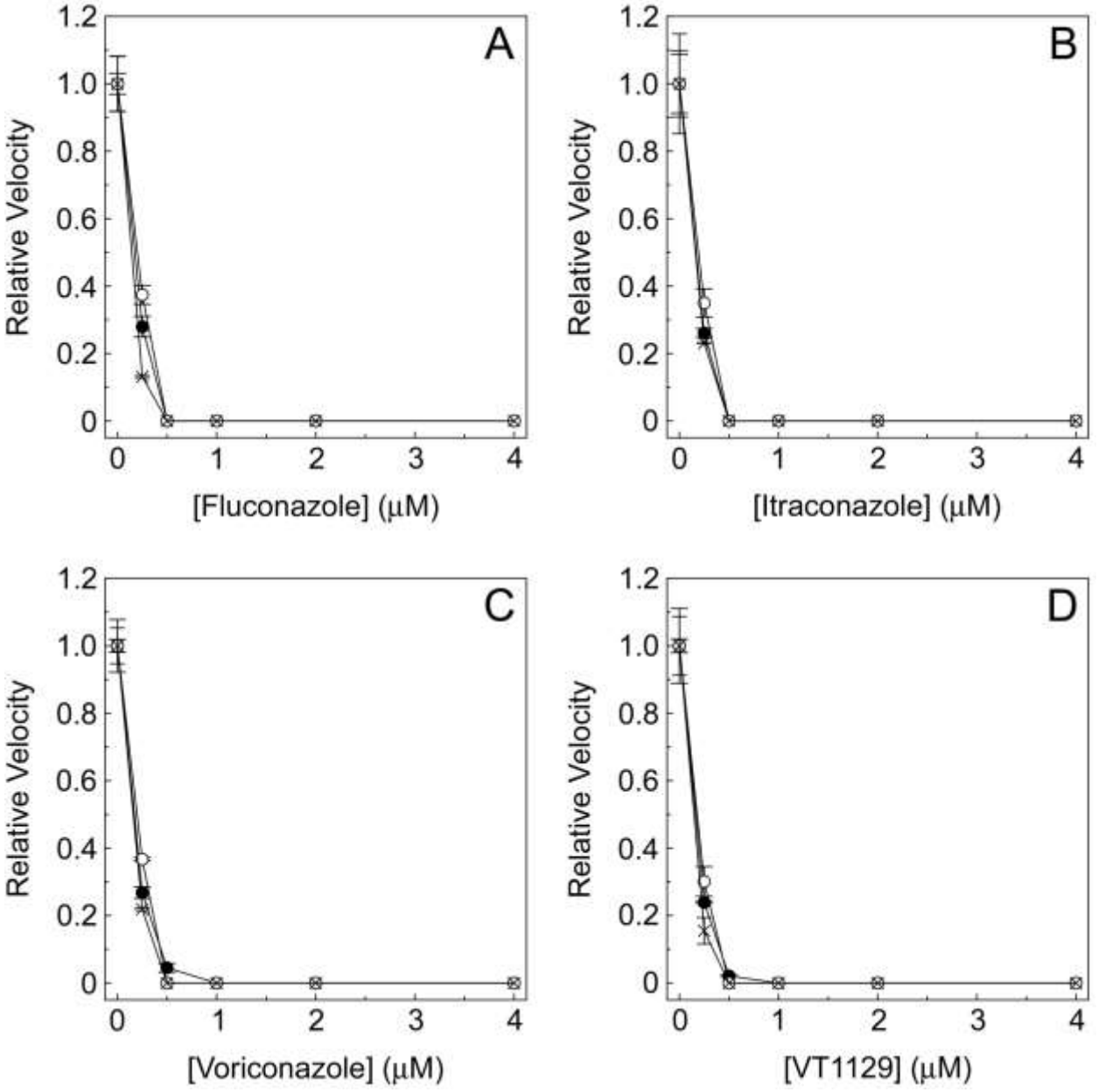

FIG 6 Azole IC_{50} determinations for cryptococcal CYP51 proteins. The IC_{50}s of fluconazole (A), itraconazole (B), voriconazole (C) and VT-1129 (D) for 0.5 μM CneoCYP51 (filled circles), CgruCYP51 (hollow circles) and CgatCYP51 (crosses) were determined using the CYP51 reconstitution assay with 1 μM AfCPR1 as the redox partner.

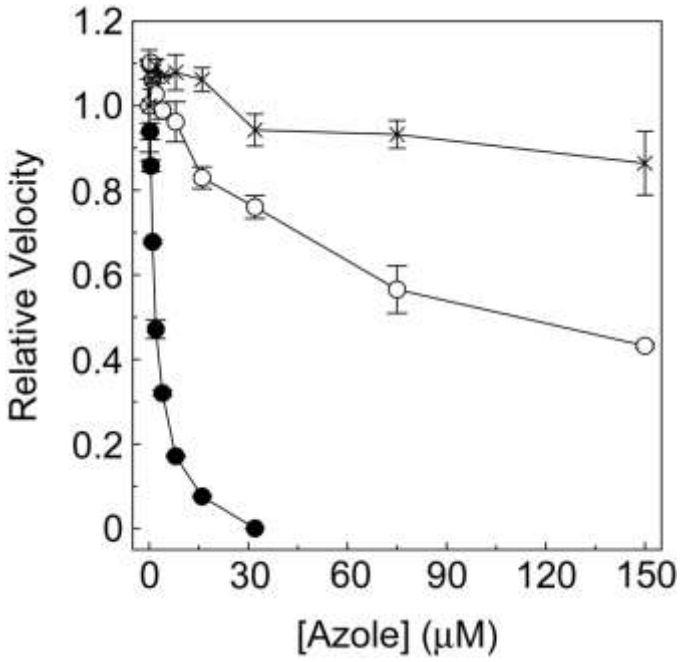

FIG 7 IC_{50} determinations with human CYP51 for clotrimazole, voriconazole, and VT-1129. The CYP51 reconstitution assay contained 0.5 μM human CYP51 and 2 μM human cytochrome P450 reductase as the redox partner in the presence of clotrimazole (filled circles), voriconazole (hollow circles), and VT-1129 (crosses) at concentrations ranging from 0 to 150 μM.